

# Rescue of skeletal muscle $\alpha$ -actin-null mice by cardiac (fetal) $\alpha$ -actin

Kristen J. Nowak,<sup>1,4</sup> Gianina Ravenscroft,<sup>1,2,4</sup> Connie Jackaman,<sup>1,4</sup> Aleksandra Filipovska,<sup>1,4</sup> Stefan M. Davies,<sup>1,4</sup> Esther M. Lim,<sup>1,4</sup> Sarah E. Squire,<sup>5,6</sup> Allyson C. Potter,<sup>5,6</sup> Elizabeth Baker,<sup>7</sup> Sophie Clément,<sup>8</sup> Caroline A. Sewry,<sup>9</sup> Victoria Fabian,<sup>10,11</sup> Kelly Crawford,<sup>12</sup> James L. Lessard,<sup>12</sup> Lisa M. Griffiths,<sup>10,11</sup> John M. Papadimitriou,<sup>3</sup> Yun Shen,<sup>1,4</sup> Grant Morahan,<sup>1,4</sup> Anthony J. Bakker,<sup>2</sup> Kay E. Davies,<sup>5,6</sup> and Nigel G. Laing<sup>1,4</sup>

<sup>1</sup>Centre for Medical Research, <sup>2</sup>Discipline of Physiology, School of Biomedical, Biomolecular, and Chemical Sciences, and <sup>3</sup>School of Pathology and Laboratory Medicine, The University of Western Australia, Perth, Western Australia 6009, Australia

<sup>4</sup>Western Australian Institute for Medical Research, Nedlands, Western Australia 6009, Australia

<sup>5</sup>Medical Research Council Functional Genetics Unit and <sup>6</sup>Department of Physiology, Anatomy, and Genetics, University of Oxford, Oxford OX1 2JD, England, UK

<sup>7</sup>PathWest Department of Cytogenetics, King Edward Memorial Hospital, Perth, Western Australia 6008, Australia

<sup>8</sup>Department of Pathology and Immunology, University Medical Center, University of Geneva, 1211 Geneva 4, Switzerland

<sup>9</sup>Wolfson Centre for Inherited Neuromuscular Diseases, Robert Jones and Agnes Hunt Orthopaedic and District Hospital, Oswestry SY10 7AG, England, UK

<sup>10</sup>Department of Neuropathology and <sup>11</sup>PathWest Department of Anatomical Pathology, Royal Perth Hospital, Perth, Western Australia 6001, Australia

<sup>12</sup>Division of Developmental Biology, Cincinnati Children's Hospital Medical Center, Cincinnati, OH 45229

**S**keletal muscle  $\alpha$ -actin (ACTA1) is the major actin in postnatal skeletal muscle. Mutations of ACTA1 cause mostly fatal congenital myopathies. Cardiac  $\alpha$ -actin (ACTC) is the major striated actin in adult heart and fetal skeletal muscle. It is unknown why ACTC and ACTA1 expression switch during development. We investigated whether ACTC can replace ACTA1 in postnatal skeletal muscle. Two ACTC transgenic mouse lines were crossed with *Acta1* knockout mice (which all die by 9 d after birth). Offspring resulting from the cross with

the high expressing line survive to old age, and their skeletal muscles show no gross pathological features. The mice are not impaired on grip strength, rotarod, or locomotor activity. These findings indicate that ACTC is sufficiently similar to ACTA1 to produce adequate function in postnatal skeletal muscle. This raises the prospect that ACTC reactivation might provide a therapy for ACTA1 diseases. In addition, the mouse model will allow analysis of the precise functional differences between ACTA1 and ACTC.

## Introduction

The actins are a highly conserved protein family (89% identity between cytoskeletal actin in yeast and  $\beta$ -actin in humans; Shterline et al., 1998) that play crucial roles in cell biology, in division, motility, the cytoskeleton, and contraction. Higher eukaryotes have six different actins, each expressed from separate genes (Vandekerckhove and Weber, 1978), with most variability between the proteins occurring at their N termini (Fig. S1).  $\beta$ - and  $\gamma$ -actin are almost ubiquitously expressed and form the actin cytoskeleton. Smooth muscles express smooth muscle  $\alpha$ -actin and enteric  $\gamma$ -actin, whereas striated muscles express predominantly cardiac  $\alpha$ -actin and skeletal

muscle  $\alpha$ -actin, so named after the adult tissues in which they are abundantly found.

All isoforms, except enteric  $\gamma$ -actin (GenBank/EMBL/DDBJ accession no. NM\_001615), are known to be associated with human diseases. Mutations in cytoplasmic  $\beta$ -actin (*ACTB*; GenBank/EMBL/DDBJ accession no. NM\_001101; OMIM no. 102630) can cause neutrophil dysfunction, mental retardation, and recurrent infection (Nunoi et al., 1999) or developmental malformations, deafness, and dystonia (Procaccio et al., 2006), whereas mutations in cytoplasmic  $\gamma$ -actin (*ACTG1*; GenBank/EMBL/DDBJ accession no. NM\_001614; OMIM no. 102560) cause deafness (Zhu et al., 2003). Mutated cardiac  $\alpha$ -actin (*ACTC*;

Correspondence to Kristen J. Nowak: knowak@cyllene.uwa.edu.au

Abbreviations used in this paper: EDL, extensor digitorum longus; HSA, human skeletal muscle  $\alpha$ -actin; KO, knockout; LC, liquid chromatography; MHC, myosin heavy chain; MRM, multiple reaction monitoring; MS, mass spectrometry.

© 2009 Nowak et al. This article is distributed under the terms of an Attribution-Noncommercial-Share Alike-No Mirror Sites license for the first six months after the publication date [see <http://www.jcb.org/misc/terms.shtml>]. After six months it is available under a Creative Commons License [Attribution-Noncommercial-Share Alike 3.0 Unported license, as described at <http://creativecommons.org/licenses/by-nc-sa/3.0/>].

GenBank/EMBL/DDBJ accession no. NM\_005159; OMIM no. 102540) causes dilated (Olson et al., 1998) or hypertrophic cardiomyopathy (Mogensen et al., 1999). Mutations in smooth muscle  $\alpha$ -actin (*ACTA2*; GenBank/EMBL/DDBJ accession no. NM\_001613; OMIM no. 102620) cause thoracic aortic aneurysms and dissections (Guo et al., 2007). However, the most disease-causing mutations, >170, have been identified in skeletal muscle  $\alpha$ -actin (*ACTA1*; GenBank/EMBL/DDBJ accession no. NM\_001100; OMIM no. 102610; Sparrow et al., 2003; unpublished data). Mutations in *ACTA1* cause a range of congenital myopathies characterized pathologically by nemaline bodies, intranuclear rods, excess actin thin filaments (Nowak et al., 1999), fiber type disproportion (small type I fibers; Laing et al., 2004), and/or corelike areas (Kaindl et al., 2004). Most patients with *ACTA1* mutations have severe disease leading to death within the first year of life; the most severely affected patients are born almost completely paralyzed (Wallgren-Pettersson et al., 2004). Therefore, these diseases lead to significant distress for families. Determining the *ACTA1* mutation responsible for the disease in any given family allows accurate diagnosis and the possibility of future prenatal or preimplantation diagnosis. However, as the majority of mutations are de novo, with families not having any family history of the disease (Sparrow et al., 2003), preventing new cases arising is elusive. Pursuing therapeutic approaches for diseases caused by mutations in *ACTA1* is necessary.

Considerable research has been conducted into establishing therapies for skeletal muscle diseases, with most emphasis on Duchenne muscular dystrophy (Nowak and Davies, 2004). However, many of the approaches investigated for Duchenne muscular dystrophy are not suitable for the congenital myopathies caused by mutations in *ACTA1* (for example, readthrough of nonsense mutations and antisense-induced exon skipping) because of the paucity of nonsense mutations or the small size and lack of possible alternative splicing of *ACTA1* (Nowak, 2008). Up-regulation of an alternative gene (frequently from the same gene family, including fetal isoforms) to compensate for an absent or defective gene has been successfully used as a treatment for diseases in both animal models (Tinsley et al., 1998; Imamura et al., 2005; Peter et al., 2008) and humans (Fathallah and Atweh, 2006). Up-regulation of an alternative gene, another member of the actin gene family, may be a possible route to therapy for *ACTA1* diseases.

*ACTA1* (NCBI Protein database accession no. NP\_001091) is the major protein component of the adult skeletal muscle thin filament. It interacts with myosin in the thick filaments during muscle contraction, producing the force required for movement. *ACTC* (NCBI Protein database accession no. NP\_005150) performs a similar function in the adult heart. The striated muscle actins, *ACTA1* and *ACTC*, are in fact coexpressed in heart and skeletal muscles. *ACTC* is the predominant actin isoform in fetal skeletal muscle (Ordahl, 1986) but later is down-regulated in human skeletal muscle to low levels by birth (Ilkovski et al., 2005) and accounts for <5% of the striated actin in adult skeletal muscle (Vandekerckhove et al., 1986). In vertebrates, *ACTA1* is present in the developing heart and remains up to 20% of the striated actin of the adult heart (Vandekerckhove et al., 1986). The *ACTC* and *ACTA1* isoforms are 99% identical, varying at

only 4 aa (Fig. S1). Although the precise role of these amino acid differences is not known, they are conserved from birds to humans (Kumar et al., 1997), and it has been postulated that these differences are crucial for function in their respective adult tissues (Rubenstein, 1990).

We hypothesized that if *ACTC*, a fetal striated actin isoform in skeletal muscle, could functionally replace *ACTA1* in postnatal muscle, perhaps *ACTC* could be used in a therapeutic approach for patients with currently incurable *ACTA1* myopathies. We recently demonstrated similar *ACTC* levels in extraocular muscles to those in the heart and postulated that this underlies (at least in part) the lack of ophthalmoplegia and cardiomyopathy in even the most severely affected patients with *ACTA1* mutations (Ravenscroft et al., 2008). However, if the 4 aa by which *ACTA1* and *ACTC* differ (Fig. S1) are crucial to postnatal skeletal muscle function, altering the proportions of each in muscle might be deleterious in itself.

*Acta1* knockout (KO) mice die by postnatal day 9 (Crawford et al., 2002). To investigate the interchangeability of the two almost identical striated actin isoforms, *ACTA1* and *ACTC*, and the importance of their alternating developmental expression, we tested whether *ACTC* could functionally replace *ACTA1* in developing and adult skeletal muscle and rescue *Acta1* KO mice. We sought to establish through these experiments whether *ACTC* might be harnessed as a therapy for patients with *ACTA1* disease. We show that *ACTC* can sufficiently replace *ACTA1* in postnatal mouse skeletal muscle to allow survival to adulthood, justifying future investigation of *ACTC* as a therapeutic target for *ACTA1* diseases.

## Results

### Increased *ACTC* expression in postnatal skeletal muscle was not deleterious

Two transgenic mouse lines, *ACTC<sup>Co</sup>* and *ACTC<sup>Cr</sup>*, designed to express the human *ACTC* cDNA in postnatal skeletal muscle were created. Fluorescent in situ hybridization showed that the transgene was inserted into an autosome in the *ACTC<sup>Cr</sup>* line and into the X chromosome in the *ACTC<sup>Co</sup>* line (unpublished data). Breeding results confirmed that male *ACTC<sup>Co</sup>* mice bred with wild-type females never gave rise to *ACTC<sup>Co</sup>* male offspring.

Male *ACTC<sup>Co</sup>* mice expressed significantly more *ACTC* compared with wild-type mice in all postnatal skeletal muscles tested by immunostaining (Fig. 1 A), Western blotting ( $740 \pm 60\%$ ;  $P < 0.001$ ; Fig. 2 A), and flow cytometry (not depicted). *ACTC<sup>Cr</sup>* mice had a small but not significant increase in *ACTC* expression ( $110 \pm 22\%$ ;  $P > 0.05$ ; Figs. 1 A and 2 A). Histology, electron microscopy, and maximum specific force (measured by skinned fiber and whole-muscle contractility; unpublished data) demonstrated that skeletal muscle from *ACTC<sup>Cr</sup>* and *ACTC<sup>Co</sup>* mice was similar to wild-type (C57BL/6;CBA/Ca background, with no transgene) skeletal muscle. Therefore, the presence of *ACTC* in postnatal and adult skeletal muscle did not cause any deleterious effects. Dual-label immunohistochemistry on *ACTC<sup>Co</sup>* quadriceps (Fig. 1 B) and other muscles (not depicted) for different myosin fiber types and *ACTC* showed that *ACTC* was predominantly expressed in myosin heavy chain (MHC) IIB fibers.

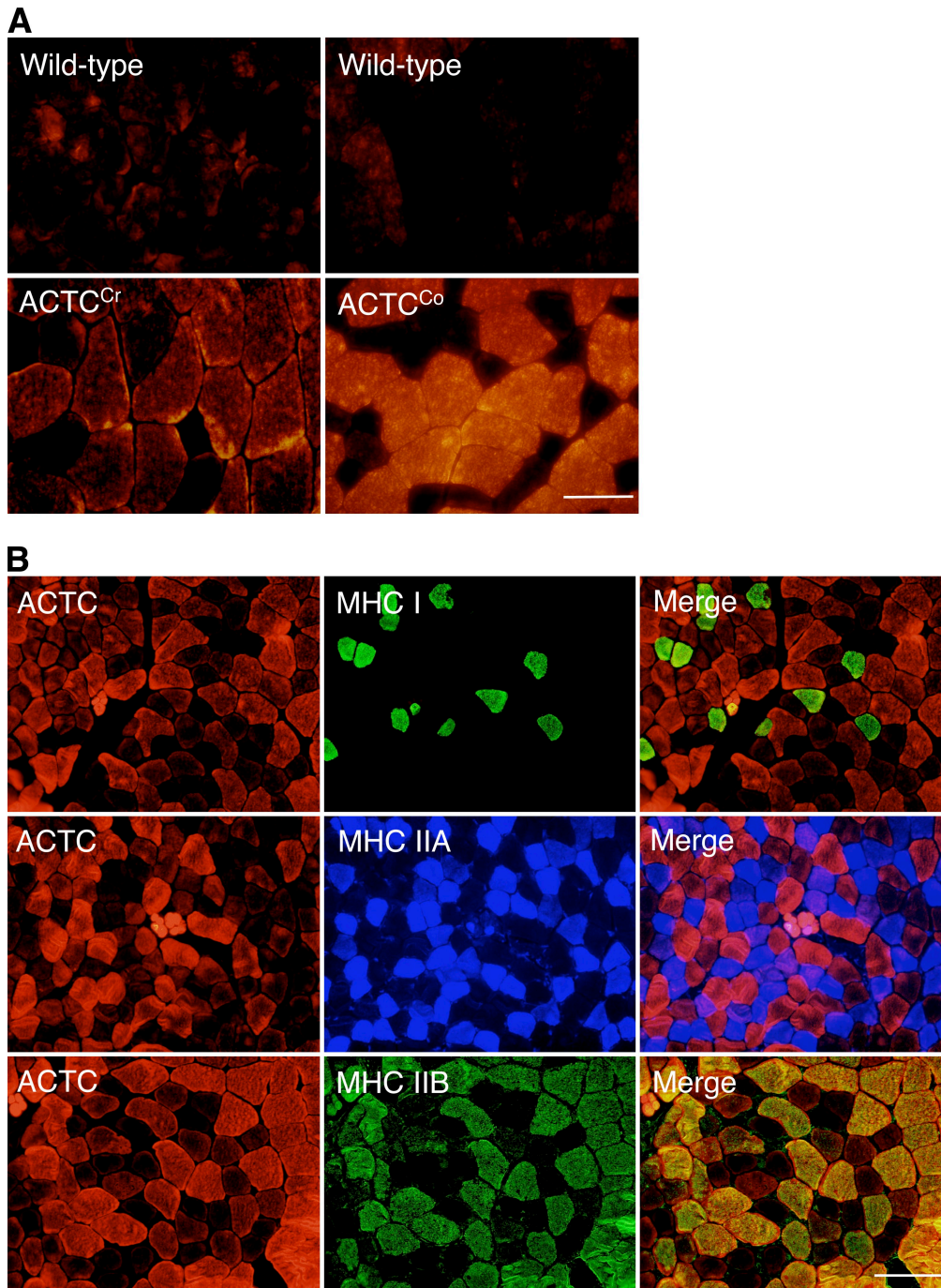


Figure 1. **Immunostaining of quadriceps muscle of 7-mo-old *ACTC* transgenic mice.** (A) ACTC staining shows that *ACTC*<sup>Co</sup> mice express more ACTC than *ACTC*<sup>Cr</sup> mice. (B) Immunostaining using ACTC and various MHC antibodies on *ACTC*<sup>Co</sup> quadriceps tissue showing that the *ACTC* transgene is predominantly expressed in MHC IIB myofibers. Bars: (A) 50  $\mu$ m; (B) 100  $\mu$ m.

#### ***ACTC* expression rescued the lethality of *Acta1* KO mice**

To investigate whether ACTC could replace ACTA1 in skeletal muscles, we crossed both *ACTC* transgenic lines with the *Acta1* KO line in which all homozygous KO mice die by 9 d after birth (Crawford et al., 2002). Crossing the higher expressing *ACTC*<sup>Co</sup> line with the *Acta1* KO mice produced 186 mice null for *Acta1* but positive for ACTC. None of these mice died within 9 d after birth, 6.5% died between 20 and 52 d,

whereas the remaining 93.5% survived for >3 mo, with the oldest alive beyond 28 mo. Crossing with the low expresser *ACTC*<sup>Cr</sup> line resulted in 61% of offspring surviving for 9 d or longer (mean age of survival, 12.5 d  $\pm$  0.536; maximum age, 20 d;  $P < 0.0001$ ). We termed the *ACTC*<sup>Co</sup>/*Acta1* KO mice *ACTC*<sup>Co</sup>/KO and performed all subsequent experiments with these mice.

The absence of ACTA1 but presence of ACTC in skeletal muscle from *ACTC*<sup>Co</sup>/KO mice was confirmed by Western blotting

**Figure 2. Protein analyses using specific ACTC and ACTA1 antibodies.** (A) Western blotting: Coomassie blue staining shows equal loading for myosin (~220 kD) for all mouse quadriceps protein samples (lanes 1 and 2 = wild-type CBA/Ca;C57BL/6, lanes 3–5 = *ACTC<sup>Cr</sup>*, lanes 6–9 = *ACTC<sup>Co</sup>*, lanes 10–13 = *ACTC<sup>Co</sup>/KO*, and lanes 14–16 = wild-type FVB/n;CBA/Ca;C57BL/6). Western blotting was performed using antibodies against total actin (all six actin isoforms; 42 kD), the striated actin isoforms only (both ACTC and ACTA1), ACTC only, or ACTA1 only. (B) Immunostaining of soleus muscles from 3-mo-old male *ACTC<sup>Co</sup>/KO* and wild-type mice using anti-ACTC (red fluorescence) and anti-ACTA1 (green fluorescence) antibodies. The arrow indicates a muscle spindle positive for ACTC. Quadriceps, gastrocnemius, and EDL muscles were also examined and showed similar results (not depicted). (C) Representative flow cytometry of myofibers dissociated from the quadriceps muscles of 9-mo-old male wild-type and *ACTC<sup>Co</sup>/KO* mice and stained using anti-ACTC and anti-ACTA1 antibodies ( $n = 12$ ). Gastrocnemius, soleus, and EDL muscles were also examined and showed similar results (not depicted). Bar, 50  $\mu$ m.

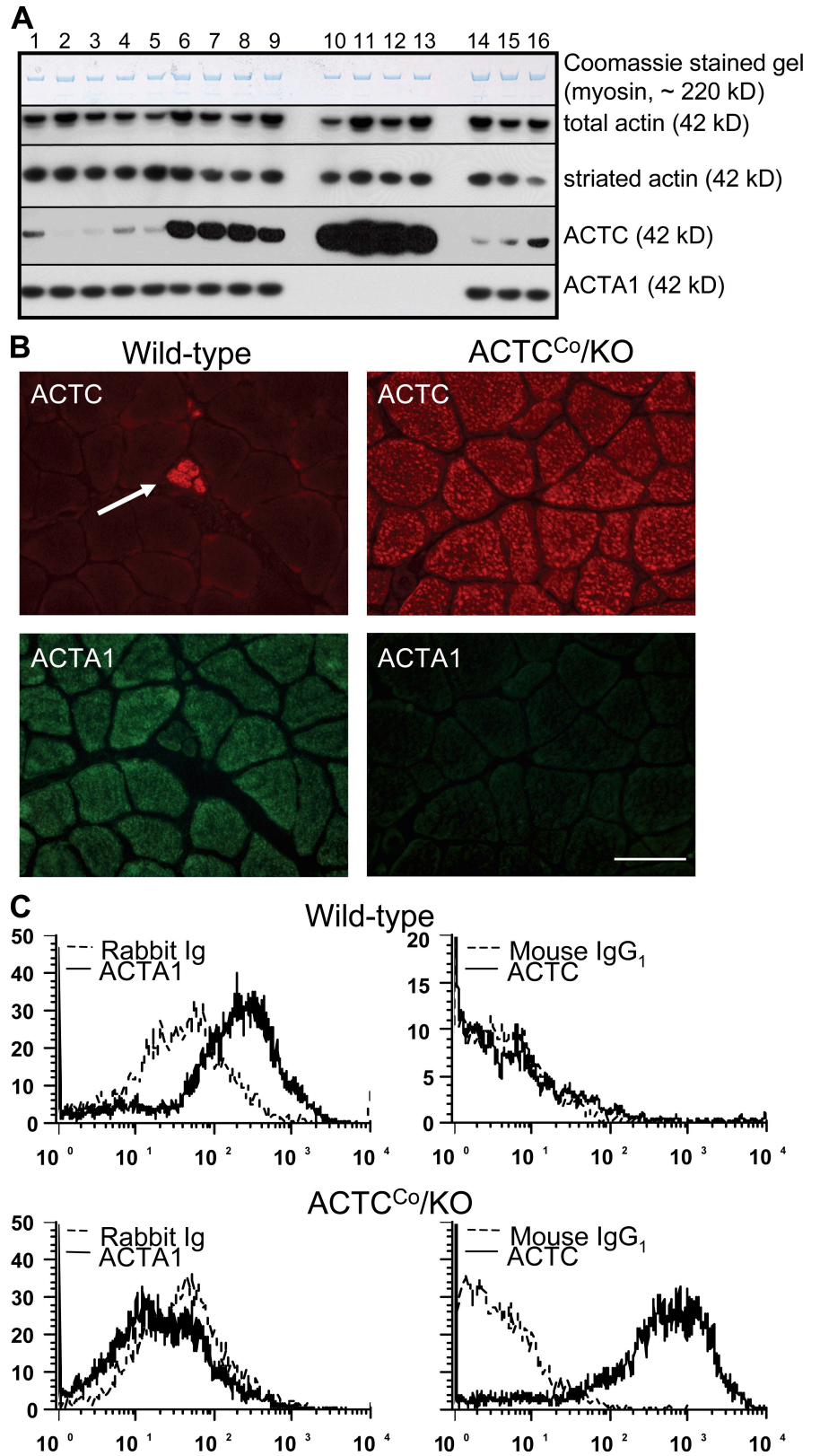


(Fig. 2 A), immunostaining (Fig. 2 B), and flow cytometry (Fig. 2 C). Liquid chromatography (LC)/tandem mass spectrometry (MS) multiple reaction monitoring (MRM) MS was used to determine the amount of ACTC present as a percentage of the total amount of striated  $\alpha$ -actin (ACTA1 + ACTC) and showed that

quadriceps muscles from *ACTC<sup>Co</sup>/KO* mice had  $99.6 \pm 0.197\%$  ACTC, whereas those from wild-type mice had  $4.26 \pm 2.57\%$  ACTC. Western blotting demonstrated similar amounts of total striated muscle  $\alpha$ -actin in the skeletal muscles of *ACTC<sup>Co</sup>/KO* and wild-type mice (Fig. 2 A).

Table I. Mass, length, body mass index measurements, and ratios of adipose tissues or EDL muscles to whole-body mass for 5.5-mo-old *ACTC<sup>Co</sup>/KO* and wild-type male mice

Measurement	Wild type	<i>ACTC<sup>Co</sup>/KO</i>
Body mass (g)	30.5 ± 0.8	22.2 ± 1.3 <sup>a</sup>
Body length (cm)	10.0 ± 0.2	8.8 ± 0.2 <sup>a</sup>
Body mass index	0.30 ± 0.01	0.29 ± 0.01
White adipose tissue		
Total (mg)	602 ± 115	226 ± 23 <sup>b</sup>
Subcutaneous (mg)	103 ± 16	80 ± 7
Epididymal (mg)	431 ± 96	125 ± 15 <sup>b</sup>
Perirenal (mg)	68.6 ± 16.7	21.5 ± 1.3 <sup>b</sup>
Ratio of epididymal + perirenal adipose tissue (g) to body mass (g)	0.0161 ± 0.0034	0.0065 ± 0.004 <sup>b</sup>
Ratio of white adipose tissue (g) to body mass (g)	0.020 ± 0.003	0.010 ± 0.001 <sup>b</sup>
Brown adipose tissue (mg)	137 ± 20	91 ± 3
Ratio of brown adipose tissue (g) to body mass (g)	0.0045 ± 0.0007	0.0041 ± 0.0002
EDL mass (mg)	11.1 ± 0.2	12.1 ± 0.3 <sup>a</sup>
Ratio of EDL mass (mg) to body mass (g)	0.33 ± 0.01	0.40 ± 0.01 <sup>a</sup>

*n* = 5 for each group.

<sup>a</sup>*P* < 0.005.

<sup>b</sup>*P* < 0.05.

*ACTC<sup>Co</sup>/KO* mice were fertile and produced normal-sized litters even when sibs mated. When *ACTC<sup>Co</sup>/KO* females heterozygous for the *ACTC<sup>Co</sup>* transgene were bred with *ACTC<sup>Co</sup>/KO* males, approximately one quarter of the offspring died before 9 d as they were males with no copies of the *ACTC<sup>Co</sup>* transgene, the equivalent of the *Act1* KO mice on the mixed genetic background. This suggested the survival of the *ACTC<sup>Co</sup>/KO* mice was unlikely the result of the influence of one or more of the three background strains.

Homozygous *ACTC<sup>Co</sup>/KO* females were mated with *ACTC<sup>Co</sup>/KO* males such that a line was created where all offspring were negative for *Act1* but homozygous (females) or hemizygous (males) for the *ACTC* transgene. All offspring from this line survived. However *ACTC<sup>Co</sup>/KO* mice weighed significantly less than wild-type mice at both 1 and 4 mo of age (Fig. S2). *ACTC<sup>Co</sup>/KO* mice at 4–4.5 mo had ~60% less white adipose tissue relative to body weight when examining perirenal or epididymal fat (*P* < 0.05; Table I) and 50% less adipose tissue relative to body weight when comparing the sum of subcutaneous, epididymal, and perirenal fat (*P* < 0.05; Table I). However, brown adipose tissue in *ACTC<sup>Co</sup>/KO* mice was not significantly different to wild-type mice relative to body weight, nor was body mass index (Table I).

#### Skeletal muscle from *ACTC<sup>Co</sup>/KO* mice was similar to wild type

Skeletal muscle of *ACTC<sup>Co</sup>/KO* mice showed no gross abnormalities by light microscopy (Fig. 3, A–D). Ultrastructural examination showed the myofibrillar architecture and sarcomeric pattern were retained (Fig. 3, E and F), but occasional focal irregularities, breaks and mini-streaming of the Z disc were detected. Histochemical analysis of both extensor digitorum longus (EDL) and soleus muscles did not show any differences in NADH and cytochrome oxidase/succinate dehydrogenase staining between *ACTC<sup>Co</sup>/KO* and wild-type mice (Fig. 4).

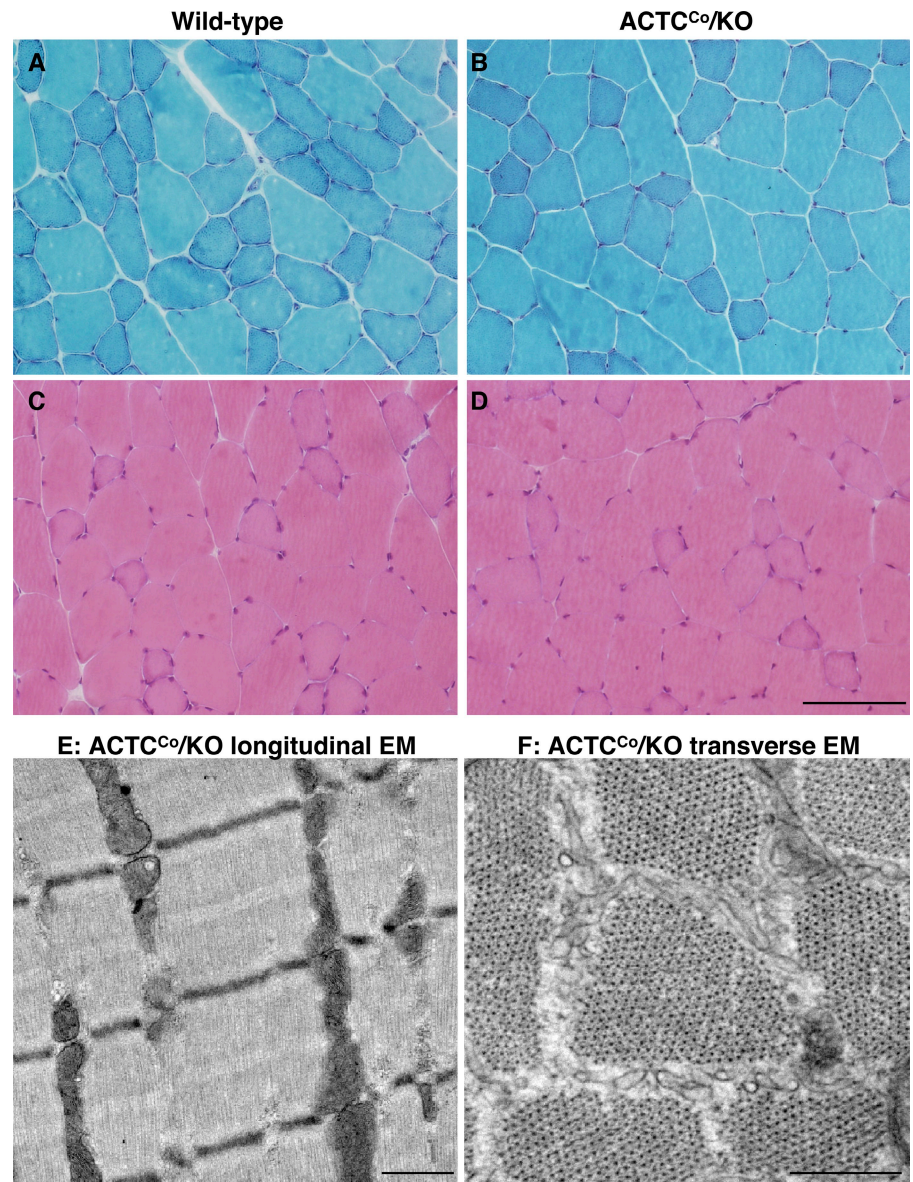
Furthermore, there were no differences in measured skeletal muscle mitochondrial function (citrate synthase, creatine kinase, and complex I) between *ACTC<sup>Co</sup>/KO* and wild-type mice (unpublished data).

Immunostaining with a variety of muscle-specific antibodies (Table S1) showed only minor differences in MHC staining, which is indicative of altered fiber-type ratios. Myofiber typing of EDL muscles (Table II) revealed that *ACTC<sup>Co</sup>/KO* mice had more MHCIIIX-positive fibers compared with wild-type mice at 4.5 mo (*P* = 0.014) and 10 mo (*P* = 0.038). However, MHCIIIX fibers were smaller at both time points (*P* = 0.046 and 0.017, respectively; Table S2). The sum of the percentages for all myosin fiber types was >100%, most likely because of the increased number of MHCIIIB/IIIX hybrid fibers in the *ACTC<sup>Co</sup>/KO* mice compared with wild-type mice (unpublished data). In the soleus muscle (Table II), *ACTC<sup>Co</sup>/KO* mice had more MHCI-positive fibers and fewer MHCIIA fibers compared with wild-type mice at 4.5 and 10 mo. Fiber sizes were similar between *ACTC<sup>Co</sup>/KO* mice and wild-type mice at both time points; only MHCIIA fibers were smaller at 4.5 mo (*P* = 0.008; Table S2).

#### Skeletal muscle from *ACTC<sup>Co</sup>/KO* mice produced slightly less specific force than wild-type muscle but had similar levels of fatigue

Both the pCa<sub>10</sub> value and slope of the pCa–force curves of 3.5-mo-old skinned EDL fibers were slightly but significantly altered for *ACTC<sup>Co</sup>/KO* (pCa<sub>10</sub> = 6.36 ± 0.017; slope = 2.55 ± 0.108) compared with wild-type mice (pCa<sub>10</sub> = 6.30 ± 0.014; slope = 2.93 ± 0.098; slope, *P* < 0.05; pCa<sub>10</sub>, *P* < 0.005; Fig. 5 A), producing a leftward shift of the force–pCa curve. However, there was no difference in the pCa<sub>50</sub> value, indicating that *ACTC<sup>Co</sup>/KO* fibers were more sensitive to lower concentrations of activating Ca<sup>2+</sup>. Normalized maximum specific force of *ACTC<sup>Co</sup>/KO* skinned EDL fibers was reduced by ~25%

Figure 3. **Histology of skeletal muscle from male *ACTC<sup>co</sup>/KO* and wild-type mice.** (A–D) Representative Gomori trichrome (A and B) and hematoxylin and eosin (C and D) staining of quadriceps muscle from 3.5-mo-old *ACTC<sup>co</sup>/KO* and wild-type mice. (E and F) Electron micrographs of quadriceps from 7-mo-old *ACTC<sup>co</sup>/KO* mice. E shows a longitudinal and F shows a cross-sectional electron micrograph. EDL and soleus muscles were also examined and produced similar results (not depicted). Bars: [A–D] 100  $\mu$ m; [E and F] 0.5  $\mu$ m.



( $21.8 \pm 1.2$  N/cm<sup>2</sup>;  $n = 23$ ) compared with wild-type mice ( $28.9 \pm 1.5$  N/cm<sup>2</sup>;  $n = 22$ ;  $P = 0.0007$ ; Fig. 5 B).

Contractility experiments were performed on isolated EDL muscles from 10-mo-old mice. The characteristics of the twitch responses were similar in wild-type and *ACTC<sup>co</sup>/KO* fibers (unpublished data). The relationship between frequency of stimulation and force was altered for *ACTC<sup>co</sup>/KO* muscle compared with wild type, with *ACTC<sup>co</sup>/KO* muscles producing significantly more relative force at 40, 60, 80, and 100 Hz of stimulation (Fig. 5 C). Overall maximal force levels of EDL muscles were similar for both groups (wild type =  $35.0 \pm 1.4$  g; *ACTC<sup>co</sup>/KO* =  $36.7 \pm 1.4$  g); however, *ACTC<sup>co</sup>/KO* EDL muscles weighed slightly more than wild-type EDL muscles ( $P < 0.0001$ ; Table I). Therefore, maximal specific force was  $\sim 15\%$  less in *ACTC<sup>co</sup>/KO* muscles ( $16.4 \pm 0.6$  N/cm<sup>2</sup>) compared with wild-type muscles ( $19.3 \pm 0.6$  N/cm<sup>2</sup>;  $P = 0.004$ ; Fig. 5 D). The susceptibility to fatigue and rate of recovery were similar for wild-type and *ACTC<sup>co</sup>/KO* muscles (Fig. 5 E).

#### ***ACTC<sup>co</sup>/KO* mice did not have a deficit in performance**

4–6-mo-old male *ACTC<sup>co</sup>/KO* mice had similar accelerating rotarod performance (Fig. 6 A) and grip strength (Fig. 6 B) compared with wild-type mice. However, when the grip strength of the *ACTC<sup>co</sup>/KO* mice was adjusted for body mass, they were 24% stronger than wild-type mice with their forelimbs (*ACTC<sup>co</sup>/KO* =  $3.578 \pm 0.1847$  g/g; wild type =  $2.89 \pm 0.1607$  g/g;  $P < 0.05$ ) and 25% stronger with all of their limbs (*ACTC<sup>co</sup>/KO* =  $5.035 \pm 0.1511$  g/g; wild type =  $4.04 \pm 0.2878$  g/g;  $P < 0.01$ ). Running wheel analysis over a 7-d period showed that maximum speed, mean speed, time spent running, and distance traveled were not decreased compared with wild-type mice (Fig. 6, C–F). In fact, the mean speed of *ACTC<sup>co</sup>/KO* mice was 31% higher than wild-type mice ( $P < 0.01$ ; Fig. 6 C), they ran 105% longer ( $P < 0.001$ ; Fig. 6 E), and, thus, they traveled 148% further ( $P < 0.001$ ; Fig. 6 F).

Locomotor analysis in an open field test also demonstrated that 4–6-mo-old *ACTC<sup>co</sup>/KO* mice were not negatively affected

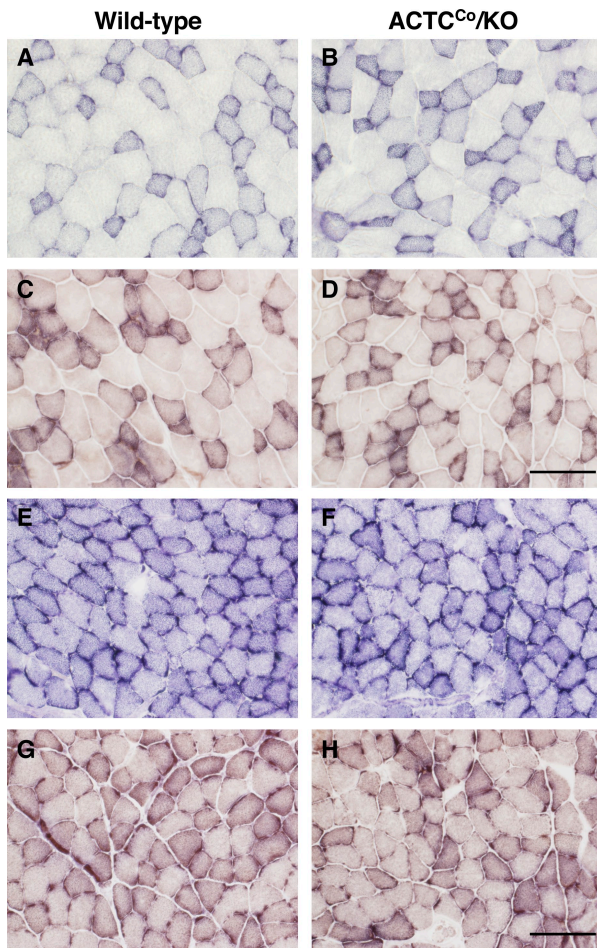


Figure 4. **Enzyme histology of skeletal muscle from male *ACTC<sup>Co</sup>/KO* and wild-type mice.** (A–H) Representative NADH (A, B, E, and F) and cytochrome oxidase/succinate dehydrogenase enzyme histology (C, D, G, and H) of EDL (A–D) and soleus (E–H) muscles from 9-mo-old *ACTC<sup>Co</sup>/KO* and wild-type mice. Bars, 100  $\mu$ m.

in terms of performance when compared with wild-type mice, but, instead, they had greater activity for all of the parameters measured when compared with wild-type mice (Fig. 7 and Video 1). *ACTC<sup>Co</sup>/KO* mice spent 9% more time moving ( $P < 0.05$ ) and at a 41% greater velocity ( $P < 0.001$ ) than wild-type mice, resulting in them traveling 41% further ( $P < 0.001$ ). *ACTC<sup>Co</sup>/KO* mice also reared more often than wild-type mice (by 126%;  $P < 0.001$ ). At older ages, 8–12 mo, when there was no longer a difference in weights between the *ACTC<sup>Co</sup>/KO* and wild-type mice, there was also no difference in running wheel activity (unpublished data).

#### Gene expression

Microarray analysis was performed to determine whether the presence of cardiac (fetal) actin induced changes in the expression levels of other muscle proteins, especially other fetal isoforms. Analysis of soleus muscles from 11-mo-old *ACTC<sup>Co</sup>/KO* mice (see Gene Expression Omnibus accession no. 12882 for all data) showed that the expression level of *Act1* was significantly decreased (log fold change =  $-4.7$ ;  $P = 2.4 \times 10^{-7}$ ), whereas that of *Actc* was significantly increased (log fold change =  $2.3$ ;  $P = 1.9 \times 10^{-4}$ ), as expected. The only other fetal skeletal muscle genes with altered expression, as measured by microarray analysis, were embryonic MHC3 (*Myh3*; log fold change =  $2.3$ ;  $P < 1.6 \times 10^{-4}$ ) and embryonic myosin light chain 4 (*Myl4*; log fold change =  $0.87$ ;  $P < 0.005$ ). In spite of this, analysis at the protein level with an antibody against Myh3 showed that there was no detectable change in Myh3 protein abundance (unpublished data). Antibodies against other candidate developmental proteins such as utrophin, fetal MHC, and cardiac troponin were used for immunostaining; no increase in their expression in *ACTC<sup>Co</sup>/KO* skeletal muscle was detected (unpublished data).

#### Discussion

We created two transgenic mouse lines, *ACTC<sup>Co</sup>* and *ACTC<sup>Cr</sup>*, which expressed ACTC in postnatal skeletal muscle. ACTC expression in the transgenic lines, despite the use of the slow

Table II. **Percentage of different MHC-typed fibers in EDL and soleus muscles from wild-type and *ACTC<sup>Co</sup>/KO* mice**

Age	Muscle	MHC fiber type	Wild type	<i>ACTC<sup>Co</sup>/KO</i>	P-value
mo			%	%	
4.5	EDL	MHCIB	67.04 $\pm$ 2.74	61.12 $\pm$ 2.97	0.124
4.5	EDL	MHCIX	31.06 $\pm$ 2.44	40.38 $\pm$ 2.44	0.014 <sup>a</sup>
4.5	EDL	MHCIIA	17.51 $\pm$ 1.05	19.64 $\pm$ 1.59	0.091
10	EDL	MHCIB	71.10 $\pm$ 4.07	74.85 $\pm$ 2.54	0.257
10	EDL	MHCIX	25.12 $\pm$ 2.40	35.08 $\pm$ 3.45	0.038 <sup>a</sup>
10	EDL	MHCIIA	20.32 $\pm$ 4.73	13.85 $\pm$ 1.80	0.537
4.5	soleus	MHCI	46.24 $\pm$ 1.21	63.54 $\pm$ 3.44	0.0002 <sup>b</sup>
4.5	soleus	MHCIIA	52.91 $\pm$ 1.62	40.04 $\pm$ 3.37	0.0021 <sup>c</sup>
10	soleus	MHCI	47.03 $\pm$ 2.98	74.97 $\pm$ 3.15	0.0095 <sup>c</sup>
10	soleus	MHCIIA	49.70 $\pm$ 3.20	22.75 $\pm$ 2.75	0.0043 <sup>c</sup>

Muscles were collected from 4.5 ( $n = 8$  or  $9$ ) and 10-mo-old ( $n = 5$ ) wild-type and *ACTC<sup>Co</sup>/KO* mice and stained with anti-MHCI, anti-MHCIIA, anti-MHCIB, and anti-MHCIX antibodies. Because of the presence of hybrid fibers expressing more than one MHC type (not depicted), the total percentage of myofibers in the EDL muscles of both types of mice is  $>100\%$ .

<sup>a</sup> $P < 0.05$ .

<sup>b</sup> $P < 0.001$ .

<sup>c</sup> $P < 0.01$ .

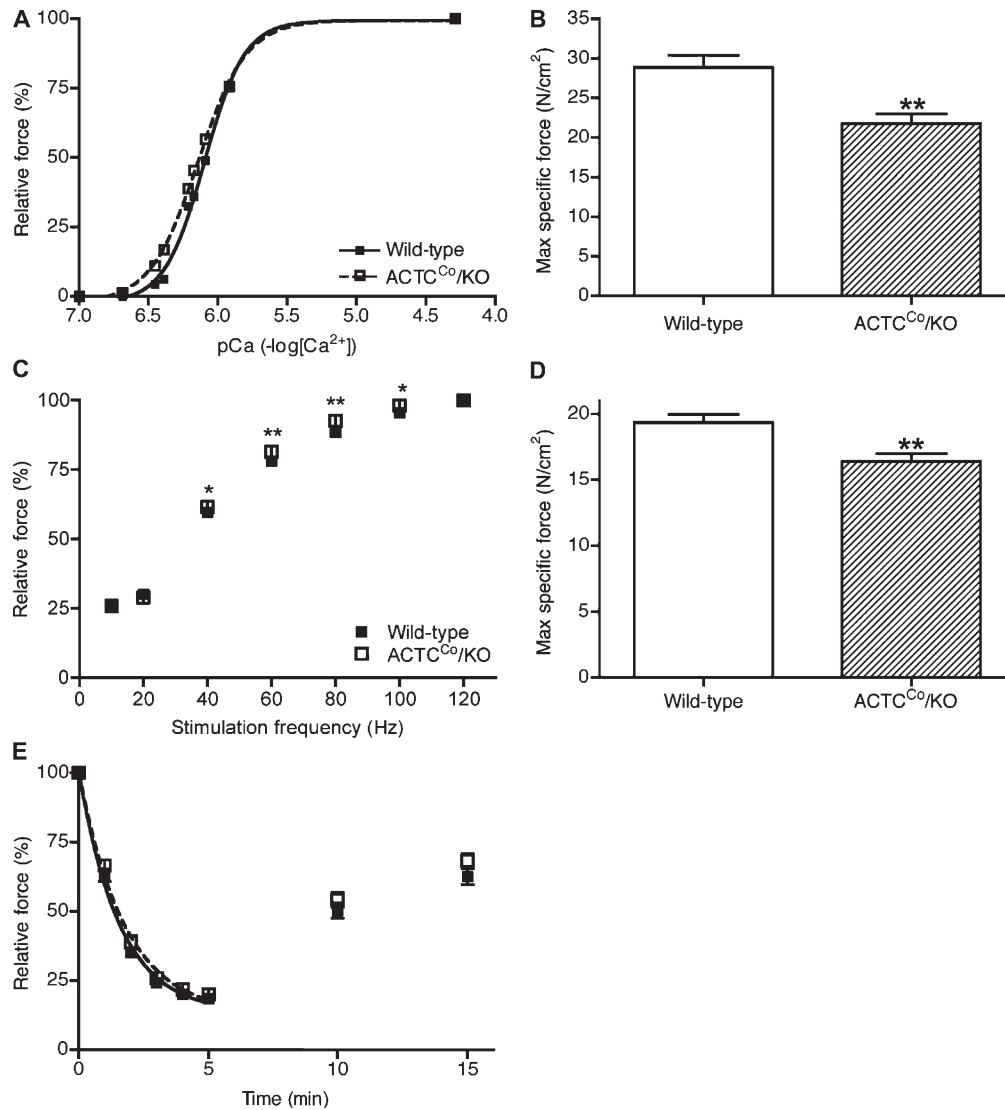


Figure 5. **Mouse physiology: individual myofiber and whole-muscle analyses.** (A and B) Skinned fiber analysis from EDL muscles from 3.5-mo-old male mice ( $n = 22$  wild type;  $n = 23$   $ACTC^{Co}/KO$ ) showing the force- $Ca^{2+}$  relationship (A) and normalized maximum force (B). (C-E) Whole EDL muscle contractile experiments from 10-mo-old male mice ( $n = 8$  for both wild-type and  $ACTC^{Co}/KO$  mice) demonstrating the force-frequency relationship (C), normalized maximal force (D), and force loss during fatiguing stimulation and postfatigue recovery (E). Error bars represent  $\pm$ SEM. \*,  $P < 0.05$ ; \*\*,  $P < 0.001$ .

troponin-I enhancer (Corin et al., 1994), was predominantly in MHCIIb fibers (Fig. 2 B), as previously reported with proteins expressed under the control of the 2.2-kb human skeletal actin promoter alone (Tinsley et al., 1996; Corbett et al., 2001; Jaeger et al., 2009). However, in the  $ACTC^{Co}/KO$  mice, ACTC expression was found in all myofiber types, presumably as a result of the absence of ACTA1. Studies have shown that there is a feedback mechanism that controls total actin levels so that strict stoichiometry of sarcomeric proteins is conserved (Kumar et al., 2004; Jaeger et al., 2009).

The lethality of the *Act1* KO mice by 9 d of age was completely overcome by the  $ACTC^{Co}$  high expressing transgene (93.5% survived well into old age). The amount of striated muscle actin in the skeletal muscles of the  $ACTC^{Co}/KO$  mice was approximately the same as that in wild-type mice. Thus, complete replacement of ACTA1 with ACTC rescued the lethal phenotype of the *Act1* KO mice. The lifespan of the *Act1* KO mice was

less dramatically extended by the  $ACTC^{Cr}$  (low ACTC expresser) transgene; 61% survived for >9 d, but the maximum age attained was only 20 d old.

The longevity of  $ACTC^{Co}/KO$  mice was unexpected. Others have shown that one actin isoform could not substitute or could only partially substitute for another. For example, cytoplasmic  $\gamma$ -actin (ACTG1) could not rescue the lethal phenotype of *Act1* KO mice, although, intriguingly, like our  $ACTC^{Co}$  and  $ACTC^{Cr}$  transgenic mice, ACTG1 could incorporate into the thin filament in transgenic mice and showed no demonstrable detrimental effect on function (Jaeger et al., 2009). Additionally, two thirds of mice with enteric  $\gamma$ -actin (ACTG2) replacing ACTC in the heart died before adulthood (Kumar et al., 1997).

It is interesting to consider the possible reasons why ACTC rescued *Act1* KO mice but ACTG1 did not. ACTA1 and ACTC differ at only 4 aa residues, whereas ACTA1 and ACTG1 differ at 24 aa residues (Fig. S1). ACTC and ACTG2 differ at only

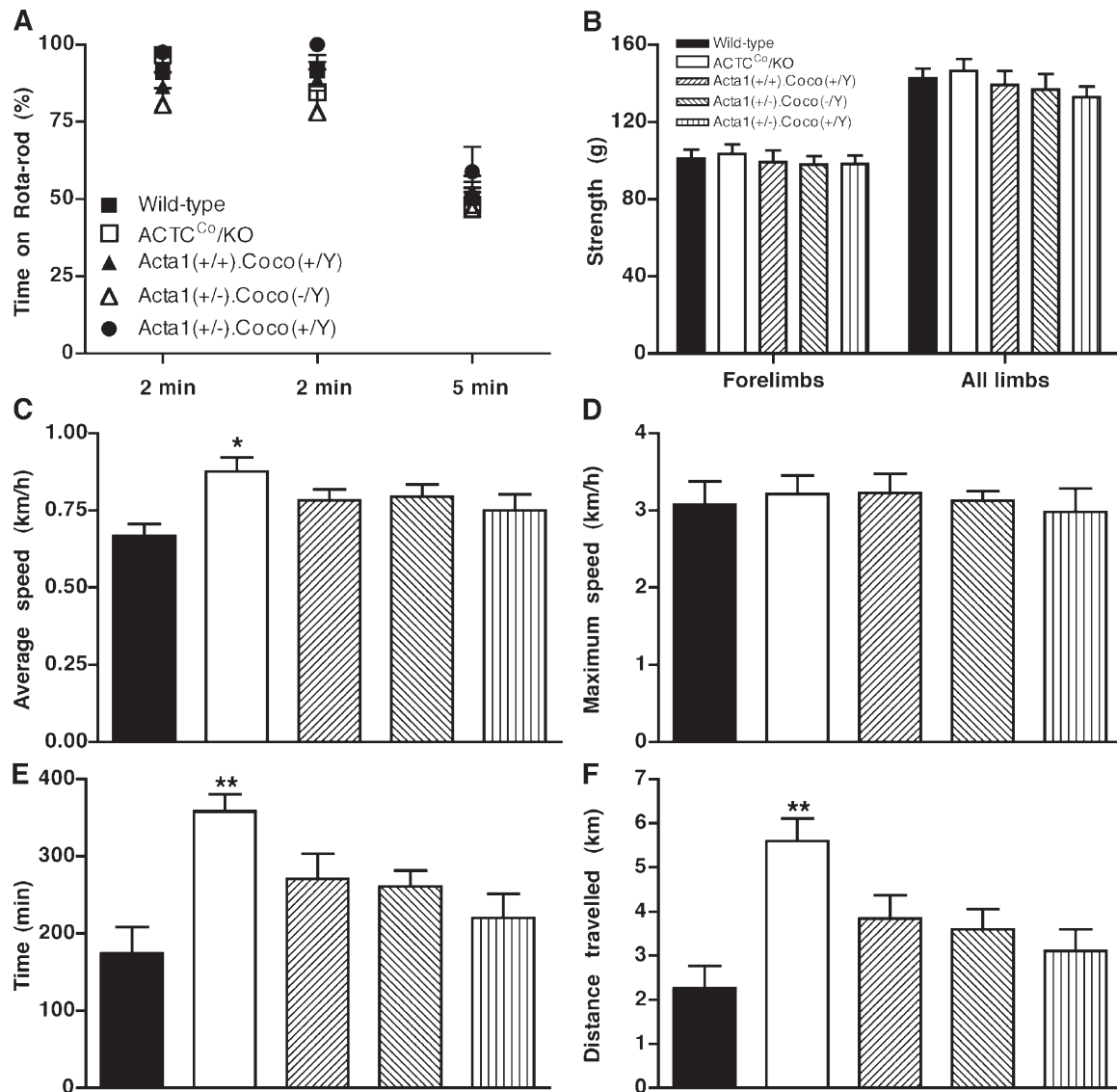


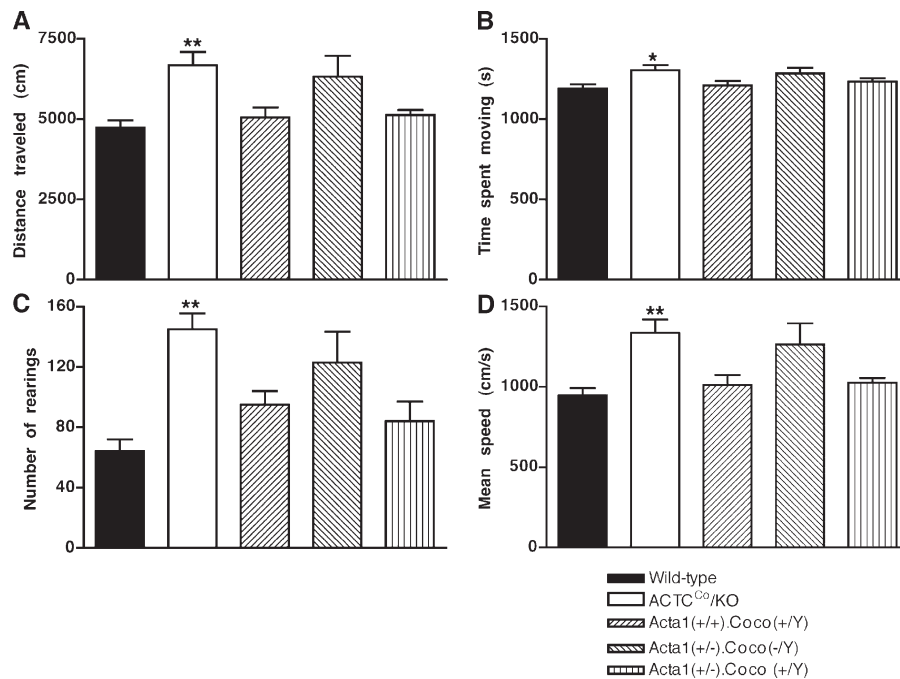
Figure 6. **ACTC<sup>Co</sup>/KO mice perform as well as or better than wild-type mice (and other genotypes tested) for grip strength, rotarod, and running wheel tests.** (A–F) Mouse performance is given as measured by rotarod (A), grip strength (B), and running wheel analysis (mean speed [C], maximum speed [D], time spent running [E], and distance traveled [F]). *n* = 10, 11, or 12 for all groups of male 4–6-mo-old mice. Error bars represent  $\pm$ SEM. \*, *P* < 0.05; and \*\*, *P* < 0.001 when ACTC<sup>Co</sup>/KO mice were compared with all other genotypes.

seven residues (Fig. S1), but it has been shown that two of those differences significantly alter the interaction of the actin isoform with myosin (Mossakowska and Strzelecka-Golaszewska, 1985). In the same experiments, it was shown that the interaction of ACTC and ACTA1 with myosin were indistinguishable (Mossakowska and Strzelecka-Golaszewska, 1985). Analysis of isolated myofibrils from cardiac muscle demonstrated a four-fold reduction in force generation compared with isolated myofibrils from skeletal muscle (Linke et al., 1994). However, these differences in force generation cannot entirely be attributed to the roles of ACTA1 and ACTC, as cardiac myofibrils also differ from skeletal muscle in other sarcomeric proteins such as troponins and tropomyosin, and a previous study has shown that cardiac and skeletal muscle troponin and tropomyosin isoforms show differences in their ability to interact with ACTA1 and myosin (Clemmens et al., 2005). Perhaps the clearest indication

of functional differences between ACTA1 and ACTC comes from the hearts of BALB/c mice, which, because of a mutation of the ACTC promoter, have reduced levels of ACTC and increased levels of ACTA1 (Jackaman et al., 2007). The hearts of BALB/c mice are hypercontractile (Hewett et al., 1994), suggesting ACTA1 generates greater force in interacting with myosin. Nevertheless, from our results, myosin and ACTC interactions generate sufficient force in the skeletal muscle sarcomere for survival, whereas ACTG1 does not.

We do not know the precise reasons for the reduced weight and size of the ACTC<sup>Co</sup>/KO mice during their early months. The difference at 1 mo must be a developmental effect and may be caused by the fact that the transgene is normally preferentially expressed in MHCIIB fibers or by the absence of ACTA1 in the developing heart or other tissues. The weight difference, including the reduction in adipose tissue, at 4 mo is probably the result

Figure 7. *ACTC<sup>Co</sup>/KO mice are more active than wild-type and other mice.* (A–D) Locomotor activity over 30 min was measured, including distance traveled (A), time spent moving (B), number of rearings (C), and mean speed (D). *n* = 10, 11, or 12 for all groups of male 4–6-mo-old mice. Error bars represent  $\pm$ SEM. \*, *P* < 0.05; and \*\*, *P* < 0.001 when *ACTC<sup>Co</sup>/KO* mice were compared with wild-type mice.



of, at least in part, the greater spontaneous activity of the *ACTC<sup>Co</sup>/KO* mice at this stage. The absence of a statistically significant difference in weight and running wheel activity later might indicate that the early differences may be more caused by effects outside of the muscle itself. For example, it is known that *ACTA1* is expressed in the brain (Bertola et al., 2008), but its function there is unknown.

The skeletal muscle in the *ACTC<sup>Co</sup>/KO* mice overall appeared normal by standard histology and electron microscopy. Some minor variations in myosin fiber types were observed in both the EDL and soleus of the *ACTC<sup>Co</sup>/KO* mice at both 4.5 and 10 mo of age (Table II), which may have been as a result of the increased activity of the *ACTC<sup>Co</sup>/KO* mice. However, there was no alteration in the levels of mitochondrial enzymes compared with wild-type mice (unpublished data). Previous studies have shown that myosin fiber types can alter without changing the levels of mitochondrial enzymes (for review see Spangenburg and Booth, 2003).

Although EDL muscles from *ACTC<sup>Co</sup>/KO* mice were larger than those from wild-type mice, this was not caused by hypertrophied muscle fibers or an increase in interstitial fat or connective tissue, as is seen with many muscular dystrophies. Despite the normalized maximum specific force for EDL muscles from *ACTC<sup>Co</sup>/KO* mice being less than wild-type mice, the overall force (taking into account the larger size of the EDL muscles) was equivalent. The increase in EDL size might be a compensatory mechanism.

Despite the exchange of *ACTA1* with the fetal/cardiac striated actin *ACTC*, no increases in the levels of the other fetal or cardiac proteins tested were detected by immunostaining. By microarray analysis, the transcriptional levels of *Myh3* and *Myl4* were significantly changed, but this could not be confirmed at a protein level for *Myh3* (*Myl4* could not be tested because of the lack of a specific antibody). Thus, it appears that

the presence of *ACTC* as the sole striated muscle  $\alpha$ -actin in skeletal muscle after birth has little influence on the levels of other muscle proteins, including other fetal proteins.

The *ACTC<sup>Co</sup>/KO* mice measured at 4–6 mo of age were not impaired in grip strength, rotarod, or locomotor activity. Despite our hypothesis that *ACTC* might replace *ACTA1* sufficiently to allow for a significant increase in survival of the resulting mice, we expected that some of these parameters of muscle function would be suboptimal, given the high evolutionary conservation of these two striated actins. However, *ACTC<sup>Co</sup>/KO* mice surprisingly showed increased activity compared with wild-type mice, for several parameters, but we cannot rule out entirely that genetic differences other than the substitution of *ACTA1* by *ACTC* are the cause of the increased activity. Nevertheless, the evidence remains that *ACTC* can function adequately in skeletal muscle during increased exercise. The large increase in the amount of voluntary exercise that the *ACTC<sup>Co</sup>/KO* mice exhibited may be the cause of the focal Z-disc abnormalities visualized by electron microscopy as such changes have been reported in endurance athletes (Grobler et al., 2004).

Among the severely affected patients with *ACTA1* mutations are those lacking *ACTA1* as the result of homozygous null mutations (Nowak et al., 2007). Most of these patients were born severely affected, with three out of seven patients requiring mechanical ventilation from birth (Nowak et al., 2007). The patient with the best clinical outcome had the highest level of *ACTC* in skeletal muscle (Nowak et al., 2007). Thus, the *ACTA1*-null patients may be overall more the equivalent of the *ACTC<sup>Co</sup>/KO* mice than the *ACTC<sup>Co</sup>/KO* mice. Therefore, our data indicate that *ACTA1*-null patients may benefit if the levels of *ACTC* in their skeletal muscles could be further increased. Experiments to ascertain whether *ACTC* expression can sufficiently dilute the effects of mutant *ACTA1* proteins are presently being performed,

as most patients with *ACTA1* disease have dominant rather than null mutations (Sparrow et al., 2003).

Our results demonstrate that ACTC can effectively replace ACTA1 in postnatal skeletal muscle. Further analysis of the *ACTC<sup>co</sup>/KO* mice will allow exploration of the precise functional differences between ACTA1 and ACTC that have led to the evolutionary development of two such similar striated muscle actins and perhaps, in time, explain their alternating expression during development.

## Materials and methods

### Mouse lines

All animal procedures were approved by the Animal Experimentation Ethics Committee of the University of Western Australia. We created two transgenic mouse lines according to standard protocols (Tinsley et al., 1996) on a C57BL/6J;CBA/Ca background, namely C57BL/6J;CBA/Ca-Tg[ACTC]CoKno (*ACTC<sup>co</sup>*; laboratory nickname "Coco") and C57BL/6J;CBA/Ca-Tg[ACTC]CrKno (*ACTC<sup>cr</sup>*; laboratory nickname "Crosby"). These lines expressed the human *ACTC* gene (identical to murine at the amino acid level) under the control of a 2.2-kb fragment of the human skeletal muscle  $\alpha$ -actin (HSA) promoter (Brennan and Hardeman, 1993) and the troponin-I slow upstream enhancer (both provided by E. Hardeman, University of New South Wales, Sydney, New South Wales, Australia; Corin et al., 1994).

To generate mice lacking *Acta1* but expressing an *ACTC* transgene, male hemizygous *Acta1* KO mice (FVB/n background) were bred with female heterozygous *ACTC* transgenic mice from each *ACTC* transgenic line. F1 offspring hemizygous for *Acta1* and heterozygous for the *ACTC* transgene were bred together to produce mice negative for *Acta1* but having one or two copies of the *ACTC* transgenes. All wild-type control animals were the mice resulting from the F1 cross homozygous for the wild-type *Acta1* allele but without a copy of the *ACTC* transgene and were thus on the same (FVB/n;C57BL/6J;CBA/Ca) genetic background.

The presence of either *ACTC* transgene was determined using primers specific for the HSA promoter (HSA forward, 5'-GATGAAGTGC-CATGATGTG-3'; and HSA reverse, 5'-TAGATGAGGCTTAGCTGGTC-3'). Genotyping for the *Acta1* wild-type and KO alleles was performed using three primers, two flanking the insertion site of the KO *PGK1* cassette (*Acta1* intron 1 forward, 5'-GCAGCGTGCCTTAATACCTC-3'; and *Acta1* intron 2 reverse, 5'-CCTGCAGATAGACATCAG-3') and the third within the *PGK1* cassette itself (*PGK1* reverse, 5'-TCCATCTGCACGACTAGT-3').

### Histology, immunostaining, fiber typing, and morphometry

10- $\mu$ m cryostat sections were stained for basic morphology and histology using standard techniques (Dubowitz and Sewry, 2007). Immunohistochemistry was performed as previously described (Jackaman et al., 2007). In brief, mouse IgG<sub>1</sub> antibodies (Table S1) were conjugated to Zenon reagents (mouse IgG<sub>1</sub>; Alexa Fluor 350, 488, or 594; Invitrogen) and incubated overnight at 4°C. IgM or rabbit IgG antibodies were incubated overnight at 4°C followed by secondary antibodies anti-mouse IgM–Alexa Fluor 488 (Invitrogen) or anti-rabbit–Alexa Fluor 488 (Invitrogen) for 45 min at RT. All slides were mounted in Hydromount (National Diagnostics) for subsequent imaging. Images were taken at RT on a fluorescent microscope (IX-71; Olympus) equipped with 20 $\times$  NA 0.45 and 40 $\times$  NA 0.60 objective lens using a digital camera (DP-71; Olympus) with DP Controller and Manager software (Olympus).

Fiber diameter was determined as the shortest distance through the center of the fiber (Briguet et al., 2004). The proportion of fibers positive for each MHC type was calculated as the percentage of positive fibers of the total fibers from two random fields containing  $\sim$ 100 fibers per field. Because of small group sizes, the Mann-Whitney test was used for statistical analysis with a 95% confidence interval.

### Electron microscopy

Excised samples were placed into fixative (2.5% cacodylate-buffered glutaraldehyde), osmicated, dehydrated in progressive alcohols and propylene oxide, and embedded in resin. Ultrathin sections were cut using an ultramicrotome (LKB 8800; Bromma), placed onto 150 mesh copper grids, and stained with acidified uranyl acetate, saturated uranyl acetate, and finally lead citrate. Grids were viewed using a transmission electron microscope

(model 2100; JEOL), and images were taken with an 11-megapixel digital camera (SC100 Orius; Gatan, Inc.).

### Western blotting

Protein extraction and Western blotting were performed essentially as previously outlined (Nowak et al., 2007). Total protein levels were measured using the bicinchoninic acid detection kit (Thermo Fisher Scientific), and 1  $\mu$ g per sample was loaded onto NuPage Novex 4–12% Bis Tris gels (Invitrogen). One gel was stained by Coomassie dye, and then the myosin bands were compared for intensity. Replicate gels were transferred onto polyvinylidene fluoride membranes using Towbin's transfer buffer (25 mM Tris, 192 mM glycine, and 20% methanol) at 300 mA for 2 h at RT. Membranes were blocked for 1 h at RT in blocking buffer (5% skim milk powder in PBS and 0.1% Tween 20) and then incubated with one of the appropriate primary antibodies (concentrations given in Table S1) overnight at 4°C in blocking buffer. Membranes were washed three times for 5 min with 0.1% Tween 20 and PBS before 1-h incubations with corresponding secondary antibodies (either HRP-conjugated goat anti-rabbit [clone A0545; Sigma-Aldrich] or HRP-conjugated rabbit anti-mouse [clone A9044; Sigma-Aldrich]), both at 1:10,000. After another set of three 5-min washes, the membranes were incubated for 5 min in ECL Plus detection reagent (GE Healthcare) and then visualized by a ChemiDoc XRS HD System (Bio-Rad Laboratories), with densitometry of ACTC-positive bands and Coomassie-stained MHC bands performed using PDQuest software (Bio-Rad Laboratories).

### MS

LC/tandem MS MRM MS was performed as previously described (Ravenscroft et al., 2008). In brief, total protein was extracted from the quadriceps from 6-mo-old male wild-type ( $n = 3$ ) and *ACTC<sup>co</sup>/KO* ( $n = 6$ ) mice and then resolved by denaturing SDS-PAGE. After Coomassie staining, proteins of the approximate size for actin (from  $\sim$ 30 to 50 kD, as actin is 42 kD) were excised from the gel, extracted, and digested using trypsin and analyzed by LC/tandem MS MRM MS. Peptides either present in both ACTC and ACTA1 proteins or specific for ACTC or ACTA1 were used to calculate the proportion of ACTC or ACTA1 of the total striated actin pool.

### Flow cytometry

Muscle flow cytometry was performed as previously described (Jackaman et al., 2007). In brief, muscle samples were incubated for 30 min in collagenase/dispase mix (each 1 mg/ml; Sigma-Aldrich) at 37°C and then prepared as a single-cell suspension by gentle dispersion using frosted glass slides followed by trituration with a Pasteur pipette. Samples were fixed in 2% paraformaldehyde for 15 min on ice and permeabilized in PBS, 10% FCS, 1% BSA, and 0.5% saponin (Sigma-Aldrich). Anti-ACTC antibody (conjugated to Zenon-XX-Biotin; Invitrogen) and anti-ACTA1 antibody were incubated overnight at 4°C. Streptavidin-R-phycoerythrin (Jackson ImmunoResearch Laboratories) and anti-rabbit–Alexa Fluor 488 (for the ACTA1 antibody; Invitrogen) were incubated for 60 min on ice. Control suspensions of relevant isotype controls, no stains, and single stains were used to determine the settings for the FACSCalibur (BD).

### Mitochondrial isolation

Muscle homogenates and mitochondria isolated from muscle were prepared principally as described previously (Frezza et al., 2007). Minced muscles were placed into 0.5% trypsin-EDTA in PBS for 30 min on ice, after which they were centrifuged at 200 g for 5 min at 4°C. The supernatant was removed, and the pellets were resuspended in 67 mM sucrose, 50 mM Tris-HCl, 50 mM KCl, 10 mM EDTA, and 0.2% BSA, pH 7.4, and then further homogenized by passing through a 70- $\mu$ m nylon cell strainer. To isolate mitochondria, muscle homogenates were centrifuged at 700 g for 10 min at 4°C, and the supernatant was further centrifuged at 8,000 g for 10 min at 4°C. The supernatant was discarded, and the pellet was resuspended in 250 mM sucrose, 3 mM EGTA, and 10 mM Tris/HCl, pH 7.4. The samples were centrifuged at 8,000 g for 10 min at 4°C before the pellet was resuspended in 150  $\mu$ l of this same buffer and then kept on ice. Mitochondria were then used to perform assays assessing citrate synthase, complex I, and creatine kinase activity. Statistical analyses were performed using Student's two-tailed *t* test with equal variance.

### Skinned fiber analysis

The contractile properties of the myofilaments were characterized using single, mechanically skinned fibers from the EDL muscles of male 3.5-mo-old *ACTC<sup>co</sup>/KO* and wild-type mice. Isometric force was measured with a sensitive force transducer (SI Heidelberg). Data were acquired using a

PowerLab data acquisition system (ADInstruments). To maximize the force production, the fibers were stretched from slack length by 20% (Han and Bakker, 2003). The sensitivity of the contractile apparatus to  $Ca^{2+}$  and maximal force production was determined by exposing the skinned fibers to solutions of different free  $Ca^{2+}$  concentrations.

#### Whole-muscle analysis

Excised EDL muscles from 10-mo-old male mice were suspended in a vertical organ bath connected to a force transducer (1200 A; Intact Muscle Test System; Aurora Scientific, Inc.). The organ bath contained carbogen (5%  $CO_2$  in oxygen) and bubbled Ringer solution (137 mM NaCl, 24 mM  $NaHCO_3$ , 11 mM glucose, 5 mM KCl, 2 mM  $CaCl_2$ , 1 mM  $NaH_2PO_4$ , and 1 mM  $MgSO_4$ ) and was maintained at 25°C. The dynamic properties of twitch response, the force–frequency relationship, susceptibility to fatigue, and rate of postfatigue recovery were all measured.

#### Phenotypic tests

Male mice were analyzed at the Integrated Neuroscience Facility (<http://www.hfi.unimelb.edu.au/inf>) for motor function according to their standard protocols. At least 10 mice from each of the five different genotypes in the age range from 4 to 6 mo were tested for grip strength, rotarod, and voluntary running wheel performance. Prism 4 software (GraphPad Software, Inc.) was used to conduct one-way analyses of variance of the phenotypic data followed by a Bonferroni post-hoc test.

#### Statistics

Data are presented as the mean  $\pm$  SEM. Prism 4 was used to conduct two-tailed *t* tests for all statistical analyses, except for the force–frequency and fatigue datasets. Multivariate analysis of variance was conducted using Statistica (StatSoft Pacific Pty. Ltd.) with main effects of genotype and repeated measures of frequency and time for the force–frequency and fatigue datasets, respectively. When the multivariate analysis of variance indicated significant main effects and interaction, individual means were compared with a Student-Newman-Keuls post-hoc test.

#### Online supplemental material

Fig. S1 shows a comparison of the amino acid sequences of the six human actins. Fig. S2 shows a comparison of the weights of the  $ACTC^{Co}/KO$  and wild-type mice at 1, 4, 7, 12, and 18 mo. Video 1 shows 1-yr-old  $ACTC^{Co}/KO$  and wild-type mice. Table S1 shows the antibodies used in this study. Table S2 shows the sizes of MHC-typed myofibers from wild-type and  $ACTC^{Co}/KO$  mice at 4.5 and 10 mo of age. Online supplemental material is available at <http://www.jcb.org/cgi/content/full/jcb.200812132/DC1>.

We gratefully thank Neal Rubinstein for providing the Myh3 antibody. We acknowledge the professional staff at the Animal Resources Centre and the Integrated Neurosciences Facility. We acknowledge the facilities and scientific and technical assistance of the Australian Microscopy and Microanalysis Research Facility at the Centre for Microscopy, Characterisation and Analysis (The University of Western Australia; supported by University, State, and Federal Government funding). MS was performed in facilities provided by the Lotterywest State Biomedical Facility/Proteomics node and the Western Australian Institute for Medical Research.

This work was supported by the National Health and Medical Research Council of Australia (C.J. Martin Fellowship #212086 [to K.J. Nowak], project grant #403941, and fellowship #403904 [to N.G. Laing]), the Association Française contre les Myopathies, the Muscular Dystrophy Association, the Medical Research Council (UK), the Ada Bartholomew Medical Research Trust, the Government of Western Australia's Medical and Health Research Infrastructure Fund, the Western Australian Institute for Medical Research, and an Australian postgraduate award (to G. Ravenscroft).

Submitted: 22 December 2008

Accepted: 30 April 2009

## References

Bertola, L.D., E.B. Ott, S. Griepisma, F.J. Vonk, and C.P. Bagowski. 2008. Developmental expression of the alpha-skeletal actin gene. *BMC Evol. Biol.* 8:166.

Brennan, K.J., and E.C. Hardeman. 1993. Quantitative analysis of the human alpha-skeletal actin gene in transgenic mice. *J. Biol. Chem.* 268:719–725.

Briguet, A., I. Courdier-Fruh, M. Foster, T. Meier, and J.P. Magyar. 2004. Histological parameters for the quantitative assessment of muscular dystrophy in the mdx-mouse. *Neuromuscul. Disord.* 14:675–682.

Clemmens, E.W., M. Entezari, D.A. Martyn, and M. Regnier. 2005. Different effects of cardiac versus skeletal muscle regulatory proteins on in vitro measures of actin filament speed and force. *J. Physiol.* 566:737–746.

Corbett, M.A., C.S. Robinson, G.F. Duglison, N. Yang, J.E. Joya, A.W. Stewart, C. Schnell, P.W. Gunning, K.N. North, and E.C. Hardeman. 2001. A mutation in alpha-tropomyosin(slow) affects muscle strength, maturation and hypertrophy in a mouse model for nemaline myopathy. *Hum. Mol. Genet.* 10:317–328.

Corin, S.J., O. Juhasz, L. Zhu, P. Conley, L. Kedes, and R. Wade. 1994. Structure and expression of the human slow twitch skeletal muscle troponin I gene. *J. Biol. Chem.* 269:10651–10659.

Crawford, K., R. Flick, L. Close, D. Shelly, R. Paul, K. Bove, A. Kumar, and J. Lessard. 2002. Mice lacking skeletal muscle actin show reduced muscle strength and growth deficits and die during the neonatal period. *Mol. Cell. Biol.* 22:5887–5896.

Dubowitz, V., and C.A. Sewry. 2007. *Muscle Biopsy: A Practical Approach*. Third edition. Elsevier, Philadelphia. 611 pp.

Fathallah, H., and G.F. Atweh. 2006. Induction of fetal hemoglobin in the treatment of sickle cell disease. *Hematology (Am. Soc. Hematol. Educ. Program)*. 58–62.

Frezza, C., S. Cipolat, and L. Scorrano. 2007. Organelle isolation: functional mitochondria from mouse liver, muscle and cultured fibroblasts. *Nat. Protoc.* 2:287–295.

Grobler, L.A., M. Collins, M.I. Lambert, C. Sinclair-Smith, W. Derman, A. St Clair Gibson, and T.D. Noakes. 2004. Skeletal muscle pathology in endurance athletes with acquired training intolerance. *Br. J. Sports Med.* 38:697–703.

Guo, D.C., H. Pannu, V. Tran-Fadulu, C.L. Papke, R.K. Yu, N. Avidan, S. Bourgeois, A.L. Estrera, H.J. Safi, E. Sparks, et al. 2007. Mutations in smooth muscle alpha-actin (ACTA2) lead to thoracic aortic aneurysms and dissections. *Nat. Genet.* 39:1488–1493.

Han, R., and A.J. Bakker. 2003. The effect of chelerythrine on depolarization-induced force responses in skinned fast skeletal muscle fibres of the rat. *Br. J. Pharmacol.* 138:417–426.

Hewett, T.E., I.L. Grupp, G. Grupp, and J. Robbins. 1994. Alpha-skeletal actin is associated with increased contractility in the mouse heart. *Circ. Res.* 74:740–746.

Ilkovski, B., S. Clement, C. Sewry, K.N. North, and S.T. Cooper. 2005. Defining alpha-skeletal and alpha-cardiac actin expression in human heart and skeletal muscle explains the absence of cardiac involvement in ACTA1 nemaline myopathy. *Neuromuscul. Disord.* 15:829–835.

Imamura, M., Y. Mochizuki, E. Engvall, and S. Takeda. 2005. Epsilon-sarcoglycan compensates for lack of alpha-sarcoglycan in a mouse model of limb-girdle muscular dystrophy. *Hum. Mol. Genet.* 14:775–783.

Jackaman, C., K.J. Nowak, G. Ravenscroft, E.M. Lim, S. Clement, and N.G. Laing. 2007. Novel application of flow cytometry: determination of muscle fiber types and protein levels in whole murine skeletal muscles and heart. *Cell Motil. Cytoskeleton.* 64:914–925.

Jaeger, M.A., K.J. Sonnemann, D.P. Fitzsimons, K.W. Prins, and J.M. Ervasti. 2009. Context-dependent functional substitution of (alpha)-skeletal actin by (gamma)-cytoplasmic actin. *FASEB J.* doi:10.1096/fj.09-129783.

Kaindl, A.M., F. Ruschendorf, S. Krause, H.H. Goebel, K. Koehler, C. Becker, D. Pongratz, J. Muller-Hocker, P. Nurnberg, G. Stoltenburg-Didinger, et al. 2004. Missense mutations of ACTA1 cause dominant congenital myopathy with cores. *J. Med. Genet.* 41:842–848.

Kumar, A., K. Crawford, L. Close, M. Madison, J. Lorenz, T. Doetschman, S. Pawlowski, J. Duffy, J. Neumann, J. Robbins, et al. 1997. Rescue of cardiac alpha-actin-deficient mice by enteric smooth muscle gamma-actin. *Proc. Natl. Acad. Sci. USA.* 94:4406–4411.

Kumar, A., K. Crawford, R. Flick, R. Klevitsky, J.N. Lorenz, K.E. Bove, J. Robbins, and J.L. Lessard. 2004. Transgenic overexpression of cardiac actin in the mouse heart suggests coregulation of cardiac, skeletal and vascular actin expression. *Transgenic Res.* 13:531–540.

Laing, N.G., N.F. Clarke, D.E. Dye, K. Liyanage, K.R. Walker, Y. Kobayashi, S. Shimakawa, T. Hagiwara, R. Ouvrier, J.C. Sparrow, et al. 2004. Actin mutations are one cause of congenital fibre type disproportion. *Ann. Neurol.* 56:689–694.

Linke, W.A., V.I. Popov, and G.H. Pollack. 1994. Passive and active tension in single cardiac myofibrils. *Biophys. J.* 67:782–792.

Mogensen, J., I.C. Klausen, A.K. Pedersen, H. Egeblad, P. Bross, T.A. Kruse, N. Gergersen, P.S. Hansen, U. Baandrup, and A.D. Borglum. 1999. Alpha-cardiac actin is a novel disease gene in familial hypertrophic cardiomyopathy. *J. Clin. Invest.* 103:R39–R43.

Mossakowska, M., and H. Strzelecka-Golaszewska. 1985. Identification of amino acid substitutions differentiating actin isoforms in their interaction with myosin. *Eur. J. Biochem.* 153:373–381.

- Nowak, K.J. 2008. Therapeutic approaches for the sarcomeric protein diseases. In *The Sarcomere and Skeletal Muscle Disease*. vol. 642. N.G. Laing, editor. Landes Bioscience, Austin, TX. 207–223.
- Nowak, K.J., and K.E. Davies. 2004. Duchenne muscular dystrophy and dystrophin: pathogenesis and opportunities for treatment. *EMBO Rep.* 5:872–876.
- Nowak, K.J., D. Wattanasirichaigoon, H.H. Goebel, M. Wilce, K. Pelin, K. Donner, R.L. Jacob, C. Hubner, K. Oexle, J.R. Anderson, et al. 1999. Mutations in the skeletal muscle alpha-actin gene in patients with actin myopathy and nemaline myopathy. *Nat. Genet.* 23:208–212.
- Nowak, K.J., C.A. Sewry, C. Navarro, W. Squier, C. Reina, J.R. Ricoy, S.S. Jayawant, A.M. Childs, J.A. Dobbie, R.E. Appleton, et al. 2007. Nemaline myopathy caused by absence of alpha-skeletal muscle actin. *Ann. Neurol.* 61:175–184.
- Nunoi, H., T. Yamazaki, H. Tsuchiya, S. Kato, H.L. Malech, I. Matsuda, and S. Kanegasaki. 1999. A heterozygous mutation of beta-actin associated with neutrophil dysfunction and recurrent infection. *Proc. Natl. Acad. Sci. USA.* 96:8693–8698.
- Olson, T.M., V.V. Michels, S.N. Thibodeau, Y.S. Tai, and M.T. Keating. 1998. Actin mutations in dilated cardiomyopathy, a heritable form of heart failure. *Science.* 280:750–752.
- Ordahl, C.P. 1986. The skeletal and cardiac alpha-actin genes are coexpressed in early embryonic striated muscle. *Dev. Biol.* 117:488–492.
- Peter, A.K., J.L. Marshall, and R.H. Crosbie. 2008. Sarcospan reduces dystrophic pathology: stabilization of the utrophin-glycoprotein complex. *J. Cell Biol.* 183:419–427.
- Procaccio, V., G. Salazar, S. Ono, M.L. Styers, M. Gearing, A. Davila, R. Jimenez, J. Juncos, C.A. Gutekunst, G. Meroni, et al. 2006. A mutation of beta-actin that alters depolymerization dynamics is associated with autosomal dominant developmental malformations, deafness, and dystonia. *Am. J. Hum. Genet.* 78:947–960.
- Ravenscroft, G., S.M. Colley, K.R. Walker, S. Clement, S. Bringans, R. Lipscombe, V. Fabian, N.G. Laing, and K.J. Nowak. 2008. Expression of cardiac alpha-actin spares extraocular muscles in skeletal muscle alpha-actin diseases—quantification of striated alpha-actins by MRM-mass spectrometry. *Neuromuscul. Disord.* 18:953–958.
- Rubenstein, P.A. 1990. The functional importance of multiple actin isoforms. *Bioessays.* 12:309–315.
- Sheterline, P., J. Clayton, and J.C. Sparrow. 1998. Actin. Fourth edition. Oxford University Press, New York. 272 pp.
- Spangenburg, E.E., and F.W. Booth. 2003. Molecular regulation of individual skeletal muscle fibre types. *Acta Physiol. Scand.* 178:413–424.
- Sparrow, J.C., K.J. Nowak, H.J. Durling, A.H. Beggs, C. Wallgren-Pettersson, N. Romero, I. Nonaka, and N.G. Laing. 2003. Muscle disease caused by mutations in the skeletal muscle alpha-actin gene (ACTA1). *Neuromuscul. Disord.* 13:519–531.
- Tinsley, J.M., A.C. Potter, S.R. Phelps, R. Fisher, J.I. Trickett, and K.E. Davies. 1996. Amelioration of the dystrophic phenotype of mdx mice using a truncated utrophin transgene. *Nature.* 384:349–353.
- Tinsley, J., N. Deconinck, R. Fisher, D. Kahn, S. Phelps, J.M. Gillis, and K. Davies. 1998. Expression of full-length utrophin prevents muscular dystrophy in mdx mice. *Nat. Med.* 4:1441–1444.
- Vandekerckhove, J., and K. Weber. 1978. At least six different actins are expressed in a higher mammal: an analysis based on the amino acid sequence of the amino-terminal tryptic peptide. *J. Mol. Biol.* 126:783–802.
- Vandekerckhove, J., G. Bugaisky, and M. Buckingham. 1986. Simultaneous expression of skeletal muscle and heart actin proteins in various striated muscle tissues and cells. A quantitative determination of the two actin isoforms. *J. Biol. Chem.* 261:1838–1843.
- Wallgren-Pettersson, C., K. Pelin, K.J. Nowak, F. Muntoni, N.B. Romero, H.H. Goebel, K.N. North, A.H. Beggs, and N.G. Laing. 2004. Genotype-phenotype correlations in nemaline myopathy caused by mutations in the genes for nebulin and skeletal muscle alpha-actin. *Neuromuscul. Disord.* 14:461–470.
- Zhu, M., T. Yang, S. Wei, A.T. DeWan, R.J. Morell, J.L. Elfenbein, R.A. Fisher, S.M. Leal, R.J. Smith, and K.H. Friderici. 2003. Mutations in the gamma-actin gene (ACTG1) are associated with dominant progressive deafness (DFNA20/26). *Am. J. Hum. Genet.* 73:1082–1091.